THE JOURNAL OF BIOLOGICAL CHEMISTRY VOL. 284, NO. 39, pp. 26978–26987, September 25, 2009

Identification and Functional Characterization of Cytoplasmic Determinants of Plasmid DNA Nuclear Import*[S]

Received for publication, June 17, 2009 Published, JBC Papers in Press, July 28, 2009, DOI 10.1074/jbc.M109.034850

Felix M. Munkonge[‡§1], Vaksha Amin[¶], Stephen C. Hyde[§‖], Anne-Marie Green[§‖], Ian A. Pringle[§‖], Deborah R. Gill[§‖], Joel W. S. Smith[‡§], Robert P. Hooley[‡§], Stefania Xenariou[‡§], Malcolm A. Ward[¶], Nicola Leeds[¶], Kit-Yi Leung[¶], Mario Chan[‡§], Elizabeth Hillery[‡§], Duncan M. Geddes[‡§], Uta Griesenbach[‡§], Edith H. Postel[**], David A. Dean[‡‡], Michael J. Dunn[§§2], and Eric W. F. W. Alton[‡§]

*From the [‡]Department of Gene Therapy, National Heart & Lung Institute, Faculty of Medicine, Imperial College London, London SW3 6LR, United Kingdom, the [§]UK Cystic Fibrosis Gene Therapy Consortium and [¶]Proteome Sciences plc, South Wing Laboratory, Institute of Psychiatry, King's College London, London SE5 8AF, United Kingdom, the [‖]Nuffield Department of Clinical Laboratory Sciences, John Radcliffe Hospital, University of Oxford, Oxford OX3 0NR, United Kingdom, the **Department of Pediatrics, Robert Wood Johnson Medical School/UMDNJ, New Brunswick, New Jersey 08903-0019, the [‡‡]Division of Neonatology, School of Medicine and Dentistry, University of Rochester, Rochester, New York 14642, and the [§§]Proteome Research Centre, UCD Conway Institute of Bimolecular and Biomedical Research, University College Dublin, Belfield, Dublin 4, Ireland*

Import of exogenous plasmid DNA (pDNA) into mammalian cell nuclei represents a key intracellular obstacle to efficient non-viral gene delivery. This includes access of the pDNA to the nuclei of non-dividing cells where the presence of an intact nuclear membrane is limiting for gene transfer. Here we identify, isolate, and characterize, cytoplasmic determinants of pDNA nuclear import into digitonin-permeabilized HeLa cells. Depletion of putative DNA-binding proteins, on the basis of their ability to bind immobilized pDNA, abolished pDNA nuclear import supporting the critical role of cytoplasmic factors in this process. Elution of pDNA-bound proteins, followed by two-dimensional sodium dodecyl polyacrylamide gel electrophoresis identified several candidate DNA shuttle proteins. We show that two of these, NM23-H2, a ubiquitous c-Myc transcription-activating nucleoside diphosphate kinase, and the core histone H2B can both reconstitute pDNA nuclear import. Further, we demonstrate a significant increase in gene transfer in non-dividing HeLa cells transiently transfected with pDNA containing binding sequences from two of the DNA shuttle proteins, NM23-H2 and the homeobox transcription factor Chx10. These data support the hypothesis that exogenous pDNA binds to cytoplasmic shuttle proteins and is then translocated to the nucleus using the minimal import machinery. Importantly, increasing the binding of pDNA to shuttle proteins by re-engineering reporter plasmids with shuttle binding sequences enhances gene transfer. Increasing the potential for exogenously added pDNA to bind intracellular transport cofactors may enhance the potency of non-viral gene transfer.

Gene therapy is a rational candidate for the treatment of monogenic disorders such as cystic fibrosis (CF). Given the need for lifelong treatment, and the difficulties with readministration of viral vectors, non-viral approaches are being actively pursued. A number of hurdles to efficient gene transfer using this approach have been identified. These include access of the plasmid DNA (pDNA)[3] to the nuclei of terminally differentiated airway epithelial cells (1).

The transport of macromolecules across the nuclear pore complex (NPC) and into the nucleus is now well understood. The NPC is a highly selective channel allowing only the passive diffusion of molecules less than M_r ~40–60 kDa (8–9 nm). Facilitated transport of larger cargo molecules is mediated by nuclear-localizing signals (NLSs), and multiple families of soluble cognate transport factors. The latter include members of the importin-β/karyopherin-β superfamily that play a pivotal role in transporting cargo that carries classical NLSs as well as cargo with no obvious NLS. In the best understood pathway, importin-β specifically recognizes the NLS-containing import substrate proteins by means of the adapter molecule importin-α. The importin-α/β complex then translocates across the NPC via an as yet poorly understood energy-dependent mechanism, controlled by the nucleotide state of the Ras family GTPase Ran (2). As with many other essential cellular processes, the nuclear import machinery is highly redundant and a plethora of importin-α and -β receptor proteins are able to recognize and facilitate the transport of a wide variety of import substrates.

The size of pDNA and its lack of a NLS suggest it is unlikely to traverse the NPC as a free molecule. In dividing cells, the

* This work was supported, in whole or in part, by National Institutes of Health Grant HL59956 (to D. A. D.). This work was also supported by the Cystic Fibrosis Trust, UK and a Wellcome Trust Senior Clinical Fellowship (to E. W. F. W. A.).

[S] The on-line version of this article (available at http://www.jbc.org) contains supplemental data, Figs. S1–S6, and Tables S1 and S2.

[1] To whom correspondence should be addressed: Dept. of Gene Therapy, National Heart & Lung Institute, Faculty of Medicine, Imperial College London, London SW3 6LR, UK. Fax: 44-0-207-351-8340; E-mail: f.munkonge@imperial.ac.uk.

[2] Recipient of a Science Foundation Ireland Research Professorship.

[3] The abbreviations used are: pDNA, plasmid DNA; CFTR, CF transmembrane conductance regulator; NPC, nuclear pore complex; HSA, human serum albumin; FITC, fluorescein-5-isothiocyanate; PNA, peptide nucleic acid; WGA, wheat germ agglutinin; NLS, nuclear localizing signals; CLSM, confocal laser scanning microscopy; IPG, immobilized pH gradient; IEF, isoelectric focusing; MALDI-TOF, matrix-assisted laser desorption ionization/time of flight; PMF, peptide mass fingerprinting; MS/MS, tandem mass spectrometry; HPLC, high-performance liquid chromatography; FACS, fluorescence-activated cell sorting; p*I*, isoelectric points; NHE, nuclease-hypersensitive element.

nuclear envelope disassembles at the M phase of division, and is therefore not a barrier to DNA nuclear entry (3). For non-dividing cells, pDNA cyto-nucleoplasmic transport is likely to be a facilitated process that is mediated by the interaction of soluble cytoplasmic factors with the minimal nuclear transport machinery. In support of this notion, one of our laboratories has previously demonstrated that, whereas addition of purified importin-α, -β, and Ran was sufficient to support protein nuclear import, pDNA nuclear import also required complementation with purified nuclear extracts (4). Further, numerous laboratories have reported regulated delivery of functionally active pDNA at the nuclear import level. Initially, well-defined NLS signal peptide sequences were attached to therapeutic nucleic acid molecules, to circumvent the nuclear entry bottleneck (5). Overall, this approach has produced conflicting results, due to confounding factors that include the large size of the DNA molecule compared with the small peptide; masking of the peptide activity by strong interaction of the positively charged peptide with the negatively charged DNA, and modification of the physicochemical properties of the cationic lipid/plasmid complexes by the NLS peptide (6).

A second strategy to harness the nuclear import pathway and increase nuclear delivery of therapeutic DNA uses endogenous or recombinant DNA-binding NLS-containing proteins to bind and condense the pDNA (7). More recently, an alternative approach involves the inclusion of nucleotide sequences into the pDNA, which have affinity for nuclear transport-mediating cellular proteins, such as transcription factors. One of us first demonstrated this notion for pDNAs that contain the SV40 enhancer region, known to bind a variety of transcription factors (8). Further, tissue-specific promoter sequences, to permit interactions with specific transcription factors in the cytoplasm, have also been engineered into pDNAs. Thus, incorporation of the promoter for smooth muscle γ-actin, pDNA resulted in effective transport into the nucleus of smooth muscle cells and subsequent gene expression, whereas little pDNA was trafficked to the nucleus of control CV-1 cells (9). Several other workers have now also demonstrated the potential for control and/or enhancement of DNA nuclear import by genetic control elements (10–12).

Collectively the above findings provide a basis for a model in which DNA nuclear import is accomplished via interaction with DNA-binding, nuclear-targeted proteins, denoted DNA nuclear shuttle proteins, although a detailed understanding of these interactions remains to be achieved. Our goals were to identify key cytoplasmic determinants of pDNA nuclear import and to determine whether the resulting purified recombinant nuclear-targeted, DNA-binding shuttle proteins are able to reconstitute pDNA nuclear import. We have identified pDNA nuclear shuttle proteins by a combination of pDNA-affinity chromatography and proteomics and show that these can reconstitute nuclear import of fluorescent-labeled pDNA into permeabilized HeLa cells. Further, we demonstrate that insertion of binding sequences from two representative DNA shuttle proteins, NM23-H2 and the homeobox transcription factor Chx10, into reporter gene plasmids results in a significant enhancement of gene transfer.

EXPERIMENTAL PROCEDURES

Nuclear Import Assay in Digitonin-permeabilized HeLa Cells—Nuclear import into the digitonin-permeabilized HeLa cells using fluorescent-tagged protein (human serum albumin (25 μg/ml of NLS-HSA-FITC)) or fluorescent DNA (10 μg/ml of Oregon Green 488-labeled pDNA (Oregon Green/pCMVβ-DTS) as import substrate was assayed with a nuclear import reaction mix (consisting of import buffer supplemented with 1 μg/ml protease inhibitors, defatted bovine serum albumin (1 mg/ml), an ATP-regenerating system (2 mM ATP, 1 mM GTP, 10 mM creatine phosphate, 20 units/ml creatine phosphokinase, native purified exogenous HeLa cytoplasmic extract (5 mg/ml) as described previously (4, 13). Detailed experimental procedures are presented under supplemental data.

Depletion and Fractionation of pDNA Import Active Fraction from HeLa Cytoplasmic Extracts—Plasmid DNA affinity matrices were prepared by immobilizing pCMVβ-DTS (that contains the PNA target sequence), via the PNA, onto Sepharose 4B-linked PNA to prepare pCMVβ-DTS/PNA-Sepharose matrix for use in preparing pDNA-affinity columns. The experimental procedures are described under supplemental data. To deplete extracts, purified HeLa cytoplasmic extracts were passed twice over the pDNA-affinity column. Column flow-throughs were dialyzed overnight against import buffer followed by concentration using Centricon-5 microconcentration devices before the determination of pDNA nuclear import activity.

HeLa Cell Synchronization and FACS Analysis of Cell Cycle—The synchronization, arrest at the G_1/S phase and FACS analysis of the HeLa cell cycle were performed essentially as described by Al-Mohanna *et al.* (14) and are detailed under supplemental data.

DNA Nuclear Shuttle Protein Plasmids—The plasmid pCMV-βGal-DTS is based on the plasmid pCMV-βGal (Clontech, Mountain View, CA), containing the SV40 DTS sequence (8). The CHX-10 and NM23-H2 binding sequences were inserted into this plasmid using PCR and standard molecular biology methods. The SV40 DTS sequence was amplified by PCR using a common forward primer with homology for the 5′-end of the SV40 DTS (GGGTCGACCTTAAGGGATCCGGTACCTTCTGAGGCGGAA) and two different reverse primers containing either the CHX-10 (GGAAGCTTATAACCTAAGCTAATTAGTTATGCATGAATTCTTTGCAAAAGCCTAGGCCTCCAA) or the NM23-H2 (GGAAGCTTTGGGGAGGGTGGGGAGGGTGGGGAAGGTGGGGAGGAATTCTTTGCAAAAGCCTAGGCCTCCAA) binding sequences, a region homologous to the 3′-end of the SV40 DTS and suitable restriction enzymes sites for identification. PCR fragment sizes were confirmed by agarose gel analysis and purified by QiaExII gel extraction (Qiagen, Crawley, UK). The PCR fragments were then cloned using the Zero Blunt TOPO PCR Cloning (Invitrogen, Paisley, UK) and sequenced to confirm correct addition of the binding sequences to the SV40 DTS. The SV40-DTS sequence tagged with CHX-10 or NM23-H2 was then subcloned back into pCMV-βGal-DTS using appropriate restriction sites and in such a way as to replace the original SV40 DTS

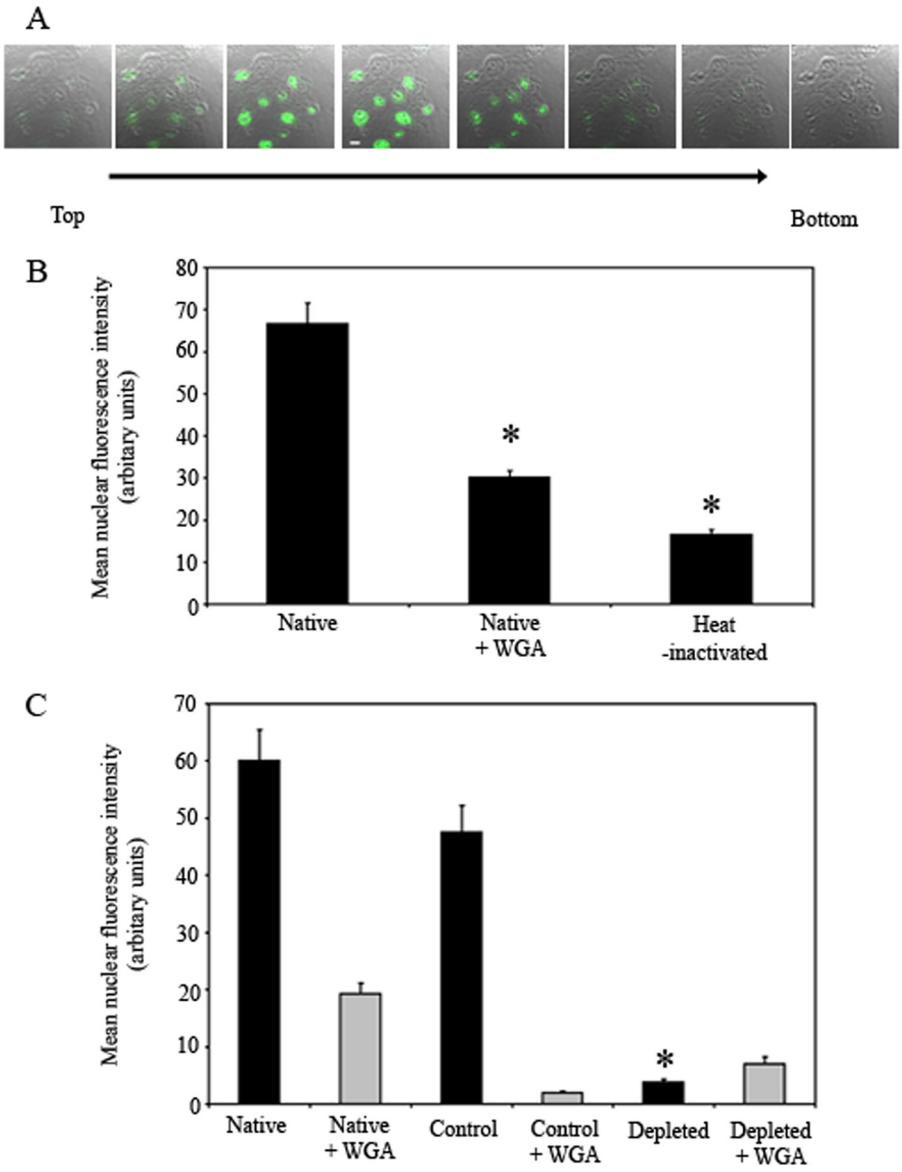

FIGURE 1. **Plasmid DNA nuclear import into digitonin-permeabilized HeLa cells.** Digitonin-permeabilized HeLa cells were incubated in the presence of recombinant importin-α, -β, and Ran, with Oregon Green/pCMVβ-DTS (10 μg DNA/ml) and native cytoplasmic HeLa (0.5 mg protein/ml). *A*, confocal z-scan consisting of 8 optical sections (0.5-μm step size) superimposed on their corresponding phase contrast images from the top to the bottom of the nuclei to verify fluorescent pDNA nuclear localization (representative of six similar experiments). *B*, quantification of the nuclear fluorescence intensity in the central sections of images from the assay performed with native (in the absence or presence of WGA) or heat-inactivated extract. The *bars* represent mean ± S.E. of the background-subtracted nuclei fluorescent intensity (n = 24–35 nuclei). Cytoplasmic extract was heat-inactivated (90 °C, 10 min) before addition. *Asterisks* indicate a significant difference from native cytoplasmic extract import activity ($p < 0.001$). *C*, depletion of putative DNA-binding factors abolishes the plasmid DNA nuclear import activity from cytoplasmic extracts. The pDNA nuclear import activity of depleted HeLa cytoplasmic extract was compared with that of native and control extracts. Digitonin-permeabilized HeLa cells were incubated with the extracts (5 mg protein/ml) containing the Oregon Green/pCMVβ-DTS (10 μg/ml) in the absence (*dark bars*) or presence (*gray bars*) of WGA (100 μg/ml). After incubation, cells were processed for visualization by CLSM. Quantification of the nuclear fluorescence intensity in central sections is shown. 17–42 nuclei were analyzed for each experimental condition. The *bars* represent mean ± S.E. of the background-subtracted nuclei fluorescent intensity compared with native cytoplasmic extract in the absence of WGA (*, $p < 0.001$).

sequence. Plasmid DNA was produced using the Qiagen Endo-Free Mega Kit (Qiagen).

Transfection of Growth-arrested HeLa Cells with Plasmid and Quantitative Analysis of β-Galactosidase Expression—The experimental procedures are described under supplemental data.

Statistical Analysis—Statistical analysis was performed using a Mann-Whitney test. Differences in β-galactosidase activity were determined using Newman-Keuls post-hoc tests after significant analysis of variance analyses on log-normalized values. The null hypothesis was rejected at $p < 0.05$. All data are presented as mean ± S.E. except where indicated.

RESULTS

Accumulation of Plasmid DNA into Nuclei of Digitonin-permeabilized HeLa Cells Requires Exogenously Added Cytoplasmic Extract—Previously we demonstrated the sequence-specific conjugation of an expression pDNA containing a 366-bp SV40 ori sequence with Oregon-Green 488-labeled peptide nucleic acid (Oregon Green/pCMVβ-DTS), while maintaining the pDNA in its native supercoiled conformation (4, 13). As previously, we assessed the nuclear accumulation of the Oregon Green-pDNA into digitonin-permeabilized HeLa cells by detection with confocal laser scanning microscopy (CLSM). As expected, the Oregon Green-pDNA accumulates in the nuclei of permeabilized HeLa cells in the presence of exogenously added cytoplasmic extract. Images representing half-micron z-axial confocal optical sections (Fig. 1*A*) indicated the *bona fide* nuclear localization of fluorescent pDNA. The Oregon Green-pDNA fluorescence displayed a punctate pattern, in comparison with the more diffuse NLS-HSA-FITC fluorescence (supplemental Fig. S1) suggesting that the exogenously added DNA may associate with specific intranuclear domains. Quantification of the nuclear-localized Oregon Green-pDNA fluorescence intensity showed that addition of the lectin wheat germ agglutinin (WGA), which specifically binds to *O*-glycosylated nuclear pore proteins, significantly ($p < 0.001$) inhibited Oregon Green-pDNA nuclear import (Fig. 1*B*), presumably due to prevention of translocation of Oregon Green-pDNA through the NPC. Consistent with our previous findings that cytoplasmic cofactors are absolutely required for pDNA nuclear import, import

activity was also significantly ($p < 0.001$) reduced by incubation with heat-inactivated cytoplasmic extract (Fig. 1*B*).

Cytoplasmic Depletion of Putative Plasmid DNA-binding Factors Abolishes Plasmid DNA Nuclear Import into Permeabilized HeLa Cells—We next asked what effect depletion of putative pDNA-binding factors from the cytoplasmic extract would have on pDNA nuclear import into permeabilized HeLa cells. After two passages through a pDNA-affinity column, comprising bait pCMVβ-DTS immobilized via a sequence-specific PNA to Sepharose matrix, cytoplasmic extracts were recovered, concentrated, and assayed for nuclear import activity. Fig. 1*C* shows that the import activity of depleted cytoplasmic extract was significantly ($p < 0.001$) reduced to a level comparable with the WGA-inhibited import activity of native extract. Control extracts, purified using PNA-Sepharose columns lacking pCMVβ-DTS, retained activity comparable with that of native cytoplasmic extracts. Furthermore the activity of control extracts was WGA-inhibitable.

Fractionation of the Plasmid DNA Nuclear Import Active HeLa Cytoplasmic Fraction—As a first step in the identification of the minimal set of factors that are sufficient for pDNA nuclear import activity, we sought to isolate the fraction of the HeLa cytoplasmic extract that was active in nuclear import. This was based on its ability to bind to immobilized PNA/pCMVβ-DTS under native conditions, identical to those under which the nuclear import activity assays were conducted. Fractionation was performed using cytoplasmic extract applied to a pCMVβ-DTS/PNA-Sepharose or control PNA-Sepharose column. After extensive washing, bound proteins were eluted with a linearly increasing salt gradient (Fig. 2) and assayed for pDNA nuclear import activity. The nuclear import of PNA/pCMVβ-DTS into permeabilized cells, supported by concentrates recovered from the pCMVβ-DTS/PNA-Sepharose column, was compared with that supported by concentrates recovered from the control PNA-Sepharose column or native cytoplasmic extracts. We noted that the absolute fluorescence nuclear intensities in this set of experiments were somewhat reduced; this may be attributable to the extensive sample handling involved. Fig. 2 shows significant ($p > 0.001$) differences in nuclear import activity in the absence of WGA compared with native cytoplasmic extract activities for all groups. The pCMVβ-DTS/PNA-Sepharose elution fractions 6 and 8 were able to reconstitute pDNA import activity compared with control PNA-Sepharose elution fractions 6 and 8 in the absence of WGA.

Identification of Proteins in Plasmid DNA Nuclear Import Active Fraction by Sequence Analysis Using Mass Spectrometry—We next identified the putative DNA-binding shuttle proteins. Proteins eluted from a pDNA-affinity column where resolved using high-resolution two-dimensional SDS-PAGE and subjected to MS analysis. Pooled elution fractions from 3 column runs each were resolved on pH 3–10 and pH 6–9 two-dimensional SDS-PAGE elution gels shown in supplemental Figs. S2*D* and S3*D*, respectively. High-sensitivity silver stain was used to detect proteins spots on both elution gels owing to low levels of protein involved. Silver staining is however incompatible with MS analysis. We thus used the electrophoretic coordinates based on our silver-stained eluate fraction pH 3–10 and pH 6–9/two-dimensional SDS-PAGE gels as reference points to manually remove a total of 62 protein spots of different intensities from Coomassie Blue-stained preparative native HeLa cell cytoplasmic extract pH 3–10 and pH 6–9 two-dimensional SDS-PAGE gels, digested them using trypsin and subjected them to MS analysis. MS data obtained by either matrix-assisted laser desorption ionization/time of flight (MALDI-TOF) and liquid chromatography-tandem mass spectrometry (LC/MS/MS) were searched against SWISS-PROT and TREMBL protein databases using the Mascot data base-searching algorithm and are summarized in supplemental Table S1. MALDI-TOF peptide mass fingerprinting (PMF) unambiguously identified proteins in all 22 spots (supplemental Table S1*A*, spots 1–22) from the pH 3–10/two-dimensional SDS-PAGE and 32 of 40 spots (supplemental Table S1*B*, spots 1–40) from the pH 6–9/two-dimensional SDS-PAGE. In addition, LC/MS/MS analysis was used to obtain the amino acid sequence of peptides 8 spots from the pH 6–9 gel that were either too faint or refractory to identification by MALDI-TOF.

Supplemental Table S1 shows an overview of all the matches identified by PMF and LC/MS/MS and represents proteins in the pCMVβ-DTS/PNA-Sepharose eluate from both the pH 3–10 (*A*) and pH 6–9 (*B*) two-dimensional SDS-PAGE gels. Functional characteristics of the protein and subcellular location, as well as the number of matching peptides and percentage sequence coverage are shown. Supplemental Fig. S4*A* shows the known protein functions, with the most highly represented involving metabolism (27%) and protein fate (18%). Approximately 11% of the identified proteins were involved in structural organization, 14% in DNA synthesis and protein synthesis (5%). The highly abundant GTP-binding nuclear protein Ran represented proteins involved in nuclear transport. Proteins involved in transcription accounted for only 5% of all identified proteins.

Identification of Plasmid DNA Nuclear Shuttle Proteins—Central to our study was the identification of soluble cytoplasm/nuclear localized DNA-binding proteins possessing, either discrete NLS signal sequences, or some form of indirect nuclear targeting. Information on the DNA binding and nuclear targeting capabilities of the identified proteins was obtained from the literature, and from bioinformatics prediction using WoLF PSORT (15), DNAProt (16), and LOCtarget (17). LOCtarget includes the NLS algorithm predictNLS that searches for the prototypical monopartite SV40 large-T antigen PKKKRKV NLS and the prototypical nucleoplasmin KRPAATKKAGQAKKKK NLS. Out of the total identified proteins, only 8 (18%) of the total identified proteins fitted our criteria for putative pDNA shuttle proteins, possessing both the ability to bind DNA and possessing a nuclear targeting capacity (supplemental Table S2).

Characterization of Plasmid DNA Nuclear Accumulation and Import Activity of Representative Plasmid DNA Shuttle Proteins—We next asked whether representatives of the eight identified putative shuttle proteins possessing both DNA binding and nuclear import capacity could support pDNA import. Histone H2B was selected as a classical DNA-binding protein. NM23-H2 was selected as a well characterized non-classical DNA-binding protein that is overexpressed in cells and was

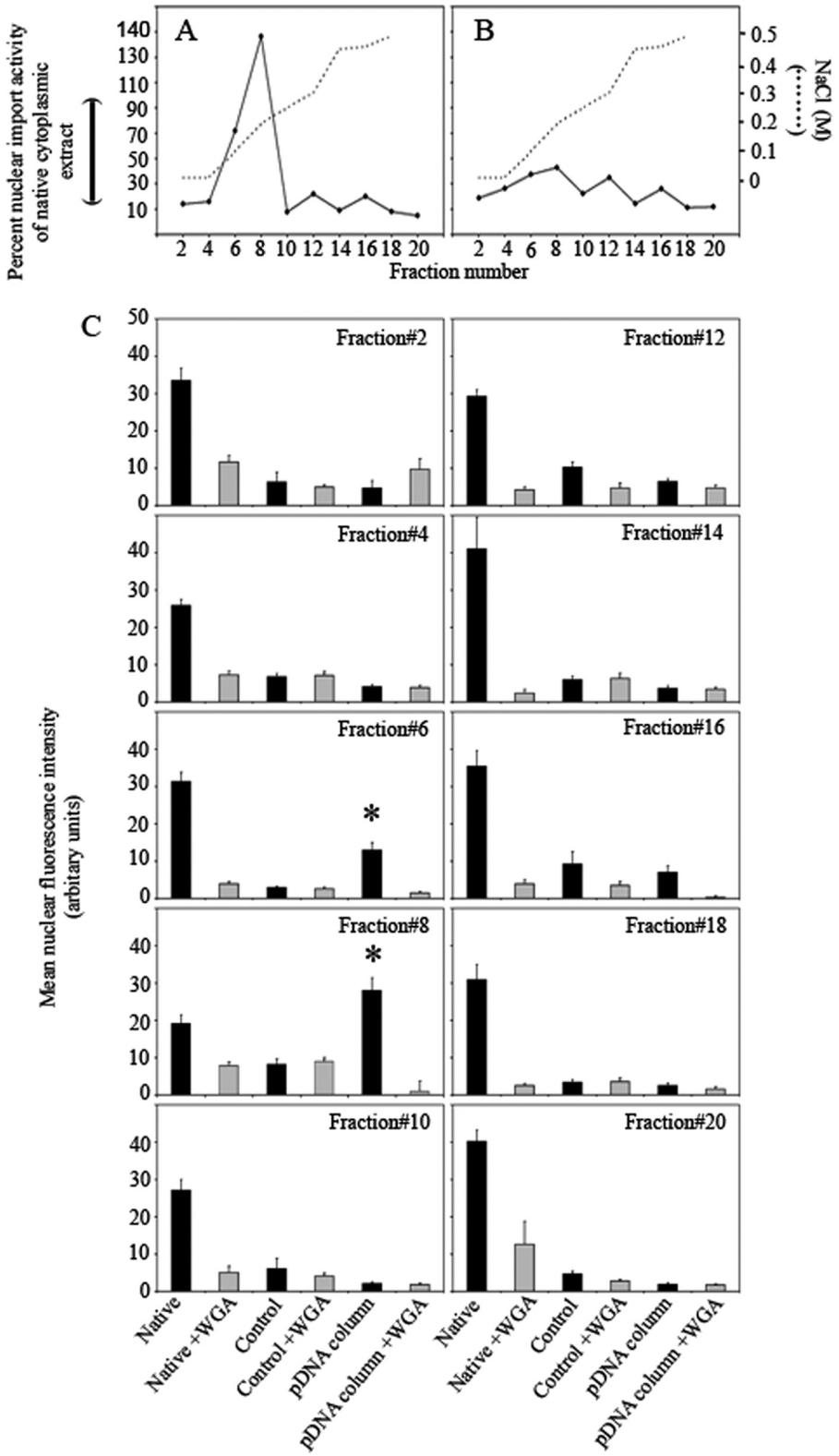

FIGURE 2. **Elution profiles of HeLa cell cytoplasmic extracts on a pCMVβ-DTS/PNA-Sepharose column.** Cytoplasmic extract (0.5 mg of protein in 500 μl) was applied to the pCMVβ-DTS/PNA-Sepharose column (*A*) or control PNA-Sepharose column (*B*), washed with three column volumes of column buffer, and elution achieved with a linear gradient of NaCl (0–0.5 M NaCl, per 20 ml buffer; 0.5 min/ml, 4 °C). Alternate elution fractions (2 ml each) were pooled (denoted numbers 2, 4, 6, 8, 10, 12, 14, 16, 18, and 20), dialyzed overnight against import buffer, concentrated using Centricon-5 microconcentration devices and assayed for Oregon Green/pCMVβ-DTS nuclear import activity. Quantification was performed on 8–59 nuclei for each type of treatment. Percent activity represents the mean background-subtracted nuclear fluorescent intensity as a percentage of the native HeLa cytoplasmic extract import activity. The concentration of the linear NaCl gradient is superimposed on the elution profile. *C*, fractionation of pDNA nuclear import activity from HeLa cell cytoplasmic extracts using the pCMVβ-DTS/PNA-Sepharose column. Details are as for *A* and *B*. Activity was determined in the absence (*dark bars*) or presence (*gray bars*) of WGA (100 μg/ml). Data points represent the mean nuclear fluorescence intensity $\pm$ S.E. ($n = 8$–59 nuclei).

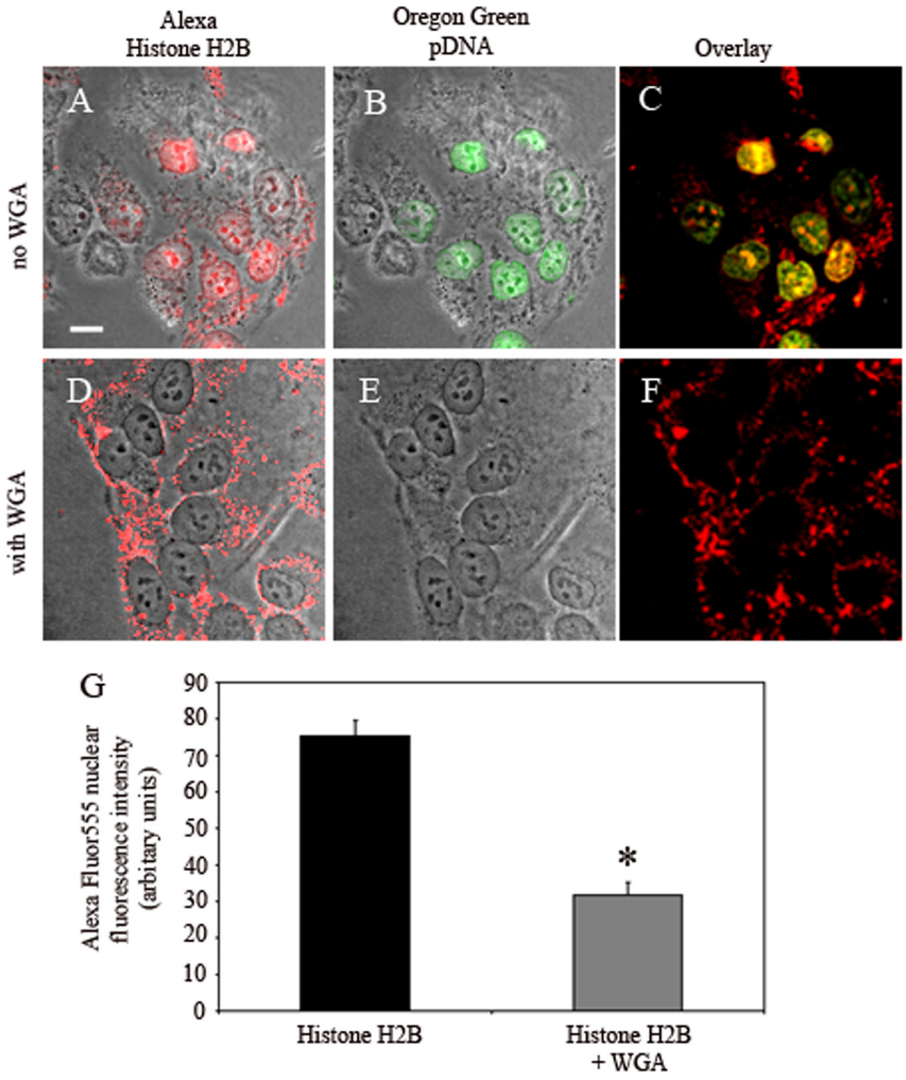

FIGURE 3. **Nuclear entry and plasmid DNA nuclear import activity of recombinant histone H2B.** Digitonin-permeabilized HeLa cells were incubated with Oregon Green/pCMVβ-DTS (10 μg/ml), cytoplasmic extract (5 mg protein/ml), and Alexa histone H2B in the absence (*A–C*) or presence (*D–F*) of WGA (100 μg/ml). After incubation, cells were processed, as indicated under "Experimental Procedures" and fluorescence images of 0.5 μm optical sections and corresponding phase contrast images visualized using a CLSM. Representative central section fluorescent images matched and superimposed with their respective phase contrast images are shown. Alexa Fluor-555 (*red*) channel; (*A*, *D*), Oregon Green 488 (*green*) channel; (*B*, *E*). Alexa Fluor 555 confocal images for histone H2B were matched to their respective Oregon Green-pDNA images, and a picture overlay was performed using Adobe Photoshop to show co-localization in the absence (*C*) or presence of WGA (*F*). *Bar*, 10 μm. *G*, quantification of the Alexa-histone H2B nuclear fluorescence intensity in the central confocal sections. The *bars* represent mean ± S.E. of the background subtracted Oregon Green/pCMVβ-DTS nuclei fluorescence intensity ($n = 33$ nuclei). The *asterisk* indicates a significant ($p < 0.001$) difference from import activity supported by recombinant importin-α, -β, and Ran alone.

readily available in our laboratories. Both were evaluated for their DNA binding capacity and nuclear import capabilities.

To assess accumulation of histone H2B into the nucleus, Alexa Fluor 555-labeled human recombinant histone H2B (Alexa-H2B) protein was incubated with the minimal import machinery consisting of recombinant importin-α, -β, and Ran, in the absence or presence of WGA, and an ATP-regenerating system. After 6 h of incubation, cells were fixed and nuclei visualized by CLSM. Fig. 3 shows that Alexa-Fluor 555 fluorescence (Fig. 3*A*) matched the corresponding nuclei in the superimposed phase image, indicating the nuclear accumulation of the Alexa-H2B. Alexa Fluor 555 rim-staining (Fig. 3*D*) indicated inhibition of the histone H2B nuclear accumulation by WGA, consistent with a previous study demonstrating the energy-dependent nuclear import of fluorescein-labeled histone H2B into permeabilized HeLa cells (18). Quantification of the Alexa-H2B nuclear fluorescence intensity (Fig. 3*G*) showed a 60% inhibition of the histone H2B nuclear accumulation by WGA ($p < 0.001$). To determine whether histone H2B functions as a pDNA nuclear shuttle protein, we performed permeabilized import assays in the presence of the minimal import pathway. Alexa-H2B was incubated with Oregon Green/pCMVβ-DTS, recombinant importin-α, -β, and RAN in the presence or absence of WGA. After 6 h, the Oregon Green/pCMVβ-DTS co-localized with the nuclear-accumulated Alexa-H2B (Fig. 3, *B* and *C*). In the presence of WGA, the nuclear accumulation of both the histone H2B and pDNA was inhibited (Fig. 3, *E* and *F*). Enhancing the brightness and contrast of the fluorescent images reveals the presence of some residual pDNA staining when the pDNA shuttle protein-nuclear import mediated by the H2B was inhibited by WGA (data not shown). Clearly, manipulating a single image within an experiment misrepresents the data and is not acceptable; therefore, the images shown in Fig. 3 are unaltered. Quantification of the Alexa-H2B nuclear accumulation, shown in Fig. 3*I*, demonstrates significant ($p < 0.001$) WGA inhibition.

As NM23-H2 lacks a discrete NLS, and its mechanism of nuclear entry is unclear we hypothesized that the constitutively expressed Hsc70, a member of the (Hsp) 70 family of molecular chaperones, plays a crucial role in the nuclear import of a subset of cytoplasmic proteins. Hsc70 possesses a NLS, has been shown to co-immunoprecipitate with a NDP kinase homologous to the NM23-H1 and -H2 isoforms in fish hepatocytes (19, 20), and facilitates entry of karyophilic proteins into digitonin-permeabilized rat kidney cells (21). In our present study, Hsc70 was identified in spot number 19 on pH 3–10/SDS-PAGE gel and we, therefore, used recombinant Hsc70 in our characterization of NM23-H2-mediated pDNA nuclear import. Alexa-NM23-H2 and Oregon Green/pCMVβ-DTS were incubated with a recombinant importin-α, -β, Ran mixture, an ATP-regenerating system and Cy5-Hsc70, and nuclear

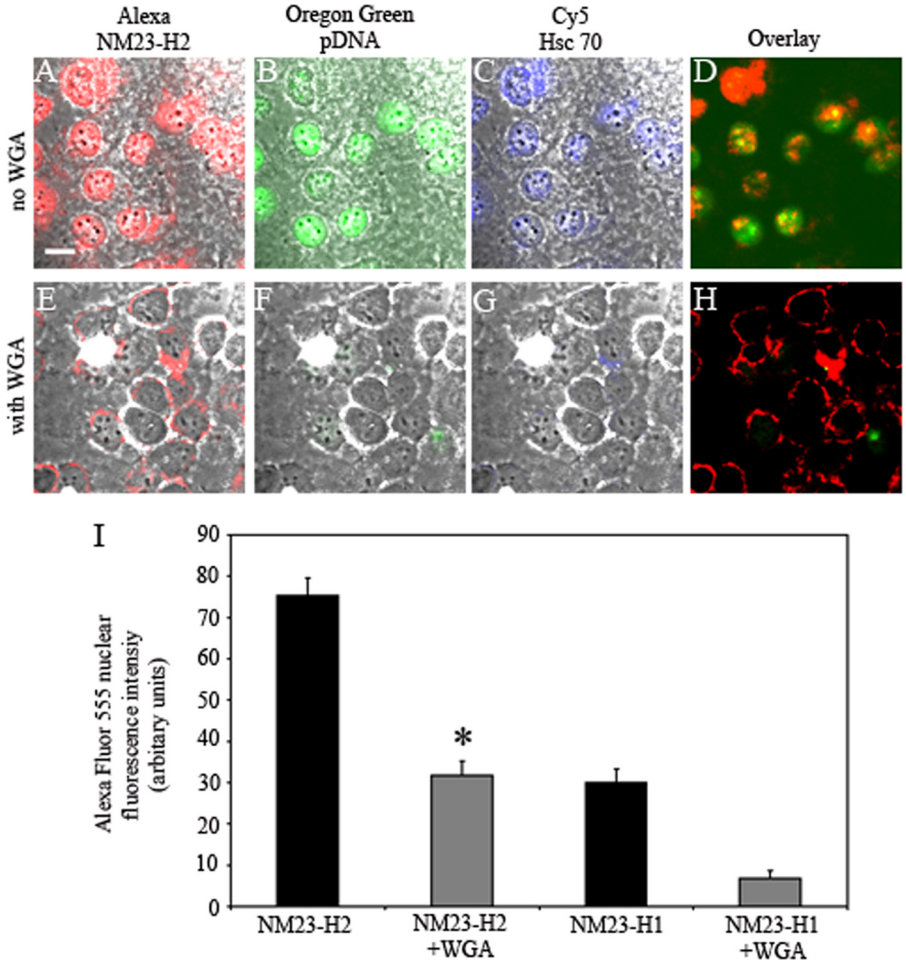

FIGURE 4. **Nuclear entry and plasmid DNA nuclear import activity of recombinant NM23-H2.** Digitonin-permeabilized HeLa cells were incubated with Oregon Green/pCMVβ-DTS, cytoplasmic extract, Cy5-Hsc70, and Alexa-NM23-H2 in the absence or presence of WGA. After incubation, cells were processed, as indicated under "Experimental Procedures," and fluorescence images of 0.5-μm optical sections and corresponding phase contrast images visualized using a CLSM. Representative central section fluorescent images matched and superimposed with their respective phase contrast images are shown. Alexa-NM23-H2 in the absence (*A–D*) or presence (*E–H*) of WGA (100 μg/ml). Alexa Fluor-555 (*red*) channel; (*A*, *E*), Oregon Green 488 (*green*) channel; (*B*, *F*), Cy-5 (*blue*) channel; (*C*, *G*). Alexa Fluor 555 confocal images for NM23-H2 were matched to their respective Oregon Green-pDNA images and a picture overlay was performed to show co-localization in the absence (*D*) or presence of WGA (*H*). *Bar*, 10 μm. *I*, quantification of the Alexa-H2B and Hsc70-mediated Alexa-NM23-H2 nuclear fluorescence intensity in the central confocal sections. *Bars* represent mean ± S.E. of the background-subtracted Oregon Green/pCMVβ-DTS nuclei fluorescence intensity (n = 33–42 nuclei). The *asterisk* indicates significant ($p < 0.001$) difference from import activity supported by recombinant importin-α, -β, and Ran alone.

accumulation of the NM23-H2 and import activity assessed after 6 h by CLSM analysis. Alexa Fluor 555 fluorescence (Fig. 4*A*) was matched to the nuclei indicating nuclear localization of the fluorescent NM23-H2. Fig. 4*E* shows perinuclear staining in the presence of WGA. Cy5-Hsc70 also accumulated in the nucleus (Fig. 4*C*), this process being inhibited by WGA (Fig. 4*G*). Quantitation of the Hsc70-mediated-nuclear accumulation of Alexa Fluor 555 fluorescence, shown in Fig. 4*I*, demonstrates that as well as an 80% inhibition by WGA ($p < 0.001$), NM23-H1 was unable to enter the nucleus either in the absence or presence of WGA.

Finally, the ability of NM23-H2 to support pDNA nuclear import was assessed by incubating Alexa-NM23-H2 with Oregon Green/pCMVβ-DTS, recombinant importin-α, -β, Ran, and Hsc70 in the presence or absence of WGA. After 6 h of incubation, Oregon Green-pDNA co-localized with the Alexa-NM23-H2 (Fig. 4, *B* and *D*). The nuclear import of the Alexa-NM23-H2/Cy5-mediated/Oregon Green-pDNA was inhibited by the addition of WGA (Fig. 4, *F* and *H*). Enhancing the Oregon Green-pDNA images in Fig. 4 shows the presence of residual pDNA staining when the pDNA nuclear import mediated by the NM23-H2 was inhibited by WGA (data not shown). As such, manipulation of single images within an experiment would misrepresent our data; the fluorescent images shown are unaltered.

Fig. 5 shows the quantification of nuclear-localized pDNA fluorescence intensity following 6 h of incubation of Oregon Green/pDNA with Alexa-NM23-H2, -NM23-H1 (with Cy-5-Hsc70), or histone H2B in the presence of recombinant importin-α, -β, and Ran compared with native cytoplasmic HeLa extract. Both NM23-H2 and histone H2B restored nuclear import activity to the levels observed for native cytoplasmic extract. Interestingly, the NM23-H1 isoform in the presence of Hsc70 was unable to reconstitute pDNA nuclear import activity and showed nuclear fluorescence intensities similar to baseline levels seen for recombinant importin-α, -β, and Ran alone.

Inserting Nuclear Shuttle Protein Sequences into pCMVβ-DTS Plasmid Enhances Reporter Gene Transfer Efficiency—We addressed the effect of incorporating binding sequences from DNA nuclear shuttle proteins on the transfer of pCMVβ-DTS in living HeLa cells. Two sequences, a 34-bp oligonucleotide making up the c-*myc* nuclease-hypersensitive element (NHE) fragment (CTCCCCACCTTCCCCACCCTCCCCAC-CCTCCCCA), and a 26-bp oligonucleotide (ATGCATAAC-TAATTAGCTTAGGTTAT) comprising the DNA-binding sequences of two representative putative shuttle proteins, (NM23-H2 and paired-type homeodomain protein Chx10, respectively (22, 23)) were inserted into the pCMVβ-DTS plasmid to produce the DNA nuclear shuttle protein plasmids pCMVβ-DTS/NM23-H2 and pCMVβ-DTS/Chx10 (Fig. 6*A*). We then compared the transfer efficiencies of these two novel plasmids with control pCMVβ-DTS in HeLa cells in culture. To test directly gene transfer in cells with intact nuclear membranes, shown here to be limiting for gene transfer in non-dividing cells, we performed gene transfer experiments in cells blocked at the G_1/S border using a combination of serum dep-

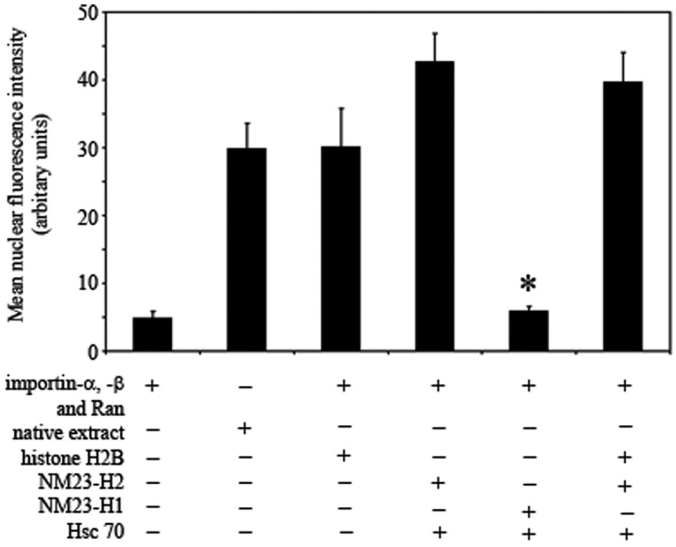

FIGURE 5. **Quantification of the Oregon Green 488-labeled pDNA nuclear fluorescence intensity in the central confocal sections is shown.** *Bars* represent mean ± S.E. of the mean background-subtracted Oregon Green/pCMVβ-DTS nuclei fluorescence intensity (n = 33–42 nuclei). The *asterisk* indicates significant ($p < 0.001$) difference from import activity supported by recombinant importin-α, -β, and Ran alone.

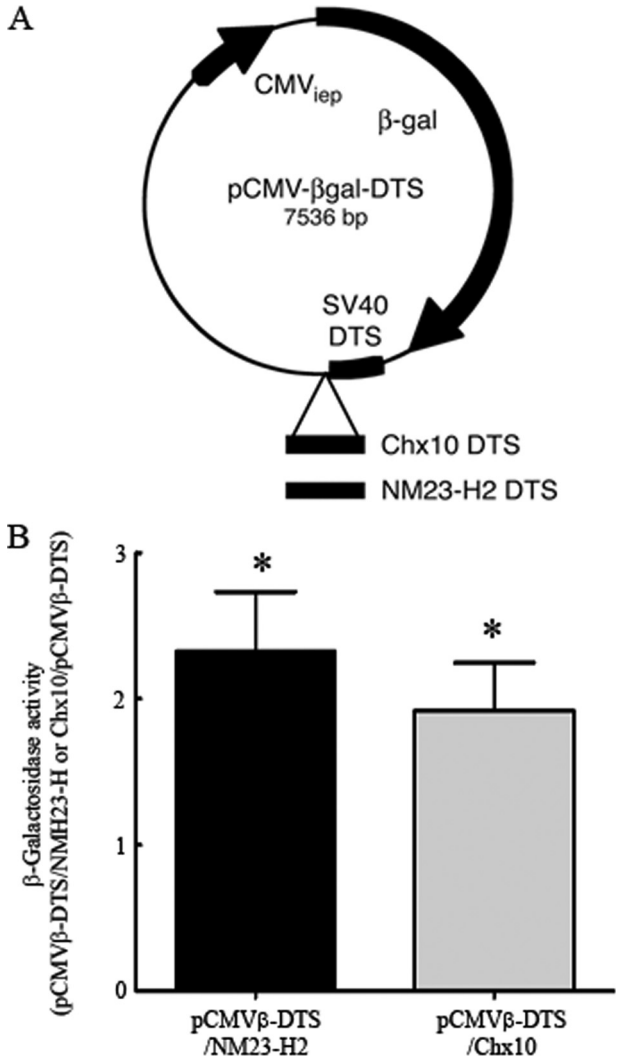

FIGURE 6. Plasmids (*A*). Abbreviated elements are as follows: *CMViep*, CMV immediate early promoter/enhancer; *Chx10* or NM23-H2, binding sequences from shuttle proteins, Chx10 and NM23-H2, respectively; *SV40 DTS*, SV40 DNA nuclear targeting sequence. β-Galactosidase reporter gene activity of pCMVβ-DTS/NM23-H2 and pCMVβ-DTS/Chx10 (*B*). Forty-eight hours after Lipofectamine 2000-mediated transfection of G_1/S-arrested HeLa cells with 1 μg of either control pCMVβ-DTS, pCMVβ-DTS/NM23-H2, or pCMVβ-DTS/Chx10, β-galactosidase activity was assayed. Data represent the mean ratio of the β-galactosidase activity (RLU/mg protein) in cells transfected with pCMVβ-DTS/NM23-H2 or pCMVβ-DTS/Chx10 and pCMVβ-DTS (means ± S.E. error bars; n = 12 dishes from three independent experiments).

rivation and aphidicolin treatment (supplemental Fig. S5). We transiently transfected G_1/S-arrested cells with 1 μg of pCMVβ-DTS/NM23-H2 or pCMVβ-DTS/Chx10 and control pDNA (pCMVβ-DTS). Forty-eight hours after transfection, the cells were harvested, and β-galactosidase specific activities measured in cell lysates using a chemiluminescent assay (supplemental data). Fig. 6*B* shows cells transfected with the two novel pDNAs showed significantly ($p < 0.05$) higher levels of β-galactosidase activity (pCMVβ-DTS/NM23-H2: 2.3 ± 0.4 and pCMVβ-DTS/Chx10: 1.9 ± 0.3; expressed as ratio of pCMVβ-DTS β-galactosidase activity) compared with cells transfected with pCMVβ-DTS. Taken together with the results demonstrating the ability of putative shuttle proteins to support pDNA nuclear import, re-engineering pDNA with shuttle protein DNA-binding sequences enhances the gene transfer ~2-fold presumably by increasing the "capture" of the pDNA by cytoplasmic-resident nuclear targeting, DNA-binding proteins.

DISCUSSION

We have identified and isolated cytoplasmic determinants of pDNA nuclear import into digitonin-permeabilized HeLa cells. We report that whereas addition of purified importin-α, -β, and Ran is sufficient to support protein nuclear import, pDNA nuclear import also requires complementation with purified cytoplasmic extract, and is WGA inhibitable. Further, we demonstrate a ~2-fold enhancement of gene transfer upon insertion of DNA binding sequences from representative DNA shuttle proteins, NM23-H2 and homeobox transcription factor Chx10, into reporter gene plasmids.

Previous investigations of plasmid nuclear entry in intact and digitonin-permeabilized cells have reported that pDNA is transported into the nucleus in association with nuclear-targeted DNA-binding proteins, such as transcription factors. Our finding that shuttle proteins within the cytoplasmic extract may be crucial for the import of DNA into nuclei of permeabilized cells is consistent with the notion that pDNA transport across the nuclear membrane follows the principles for protein import. Interestingly, the requirement for sequence specificity and protein cofactors in the nuclear import of smooth muscle cell-γ DTS (SMGA DTS) plasmid micro-injected into smooth muscle cells (SMC) has recently been demonstrated in one of our laboratories (24). This study found that binding sites for the vascular SMC-specific transcription factors serum response factor (SRF) and mammalian bagpipe homologue (NK3) where required for nuclear import. These data suggest the possibility of constructing cell-specific nuclear-targeted plasmids. Indeed, previous investigations have reported that pDNA can be translocated into the nucleus by inserting the transcription factor nuclear factor-κB (NF-κB)) binding sequences into pDNA (11,

25, 26). Here, we set out to extend the previous investigations by characterizing the nuclear-targeted DNA-binding proteins in the HeLa cytoplasmic extracts that mediate the import of pDNA into permeabilized cells. The fact that the pCMVβ-DTS/PNA-Sepharose column, but not the control PNA-Sepharose column, depleted the cytoplasmic extract suggested the feasibility of an affinity isolation approach to identify these proteins. Using a pCMVβ-DTS/PNA-Sepharose affinity column, we showed that pCMVβ-DTS/PNA-Sepharose eluates restored nuclear import activity to levels comparable with those seen for native cytoplasmic extracts.

Analysis of pDNA nuclear import active fractions by two-dimensional SDS-PAGE revealed protein spots on the elution gels representing those proteins that were enriched in the eluate fraction, presumably on the basis of their ability to bind to immobilized pCMVβ-DTS/PNA. Thus, two-dimensional SDS-PAGE produced a high-resolution protein map of the putative DNA-binding shuttle proteins. Spot analysis showed a ~4-fold reduction in complexity of the elution fraction compared with that of the native extract, control, or pDNA column flow-throughs.

We next identified proteins in the plasmid DNA nuclear import active fraction by sequence analysis using mass spectrometry. The fact that key members of the nuclear import machinery, importins-α and -β, as well as DNA-binding proteins such as common transcription factors were not detected with the proteomics approach is consistent with the well recognized caveat regarding the use of mass spectrometric analysis in conjunction with two-dimensional SDS-PAGE. Thus, while the two-dimensional SDS-PAGE separation strategy with its unique ability to resolve proteins offers a powerful qualitative tool, it biases against identification of low abundance proteins such as signaling molecules and transcription factors. Further, high abundance proteins may co-migrate and overshadow the low abundance proteins, making these difficult to detect.

Interestingly, metabolic proteins made up the majority of proteins identified in the overall spectrometric analysis. This was initially puzzling, but reports have recently suggested that several nuclear-localized glycolytic enzymes display additional moonlighting roles and carry out non-glycolytic functions (27). Moreover, some glycolytic enzymes with non-glycolytic properties, such as α-enolase (spot numbers 18 and 37 on the pH 3–10 and pH 6–9/SDS-PAGE, respectively), are known to possess evolutionarily conserved consensus *myc*-binding sites in their regulatory DNA sequences (28). The fact that proteins involved in protein fate, defense, stress and detoxification made up a significant fraction of the total protein captured by the immobilized pDNA under native conditions is not surprising. To protect themselves from oxidative stress and reactive oxygen species (ROS)-mediated protein folding, unfolding, and aggregation, cells are equipped with a variety of antioxidant proteins. Those identified in this study include peroxiredoxin 1 and molecular chaperones, such as heat shock proteins (HSP) 90. Specific effects on these mechanisms resulting from the introduction of exogenous DNA have not yet been described, but may be important to assess in future gene transfer studies. As for all proteomes, the functional concentration of proteins in the cytoplasm is in a dynamic state and proteins involved in protein fate play a key role in the regulation of protein synthesis and degradation. Ubiquitin-conjugating enzyme E2 (spot number 4, pH 3–10/SDS-PAGE) is an example of an enzyme involved in the covalent conjugation of ubiquitin to other proteins, which in turn results in the signaling of several different protein fates (29).

Characterization of pDNA nuclear accumulation and import activity of two representative pDNA shuttle proteins showed that both the histone H2B and NM23-H2, but not the control NM23-H1, were able to accumulate into the nuclei of permeabilized cells via the importin-α-/β-/Ran-dependent import pathway. Accumulation of both fluorescent-labeled recombinant proteins was WGA-inhibitable and energy-dependent. Both recombinant histone H2B and NM23-H2 were able to restore nuclear import activity to wild-type levels observed for native cytoplasmic extract in the presence of recombinant importin-α, -β, and Ran. Further, when we inserted consensus binding sequences from two representative shuttle proteins, NM23-H2, and Chx10, we were able to demonstrate an increase in gene transfer efficiency. Importantly, the observed increase in gene transfer efficiency occurred in growth-arrested (non-dividing) cells, presumably by enhancing capture and subsequent transport across the NPC by their corresponding nuclear-targeted DNA nuclear shuttle proteins.

Recently, investigations demonstrating a significant increase in transgene expression following transfection with pDNA encoding firefly luciferase possessing 5, 10, and 20 repeats of NF-κB-binding sequences inserted upstream of the CMV promoter region has been reported (26). Consistent with this finding, we show here, the insertion of a single NM23-H2 or Chx10 DNA-binding site into the reporter plasmid CMVβ-DTS increases β-Gal transgene expression significantly. Further work is needed to elucidate whether increasing the number of DNA binding sequences inserted, as well as optimizing their site placement on the pDNA further increases gene transfer above levels observed in the present study.

In conclusion, we have identified eight pDNA-bound proteins present in both the cytoplasmic and nuclear compartments, which represent a potential sink for the transport of exogenously added DNA to the nucleus. We have inserted binding sequences from the nuclear targeted-DNA binding shuttle proteins to construct plasmids that produce a significant increase in gene transfer efficiency when transfected into non-dividing cells (possessing an intact nuclear membrane barrier), presumably by enhancing translocation of pDNA across the NPC into the nucleus.

Acknowledgments—We thank Josh Gasiorowski for help with conductivity measurements and Alessandro Sardini for assistance with FACS analysis. NM23 research in the laboratory of Dr. E. H. Postel is supported by National Institutes of Health/NCI Grant R01CA076496.

REFERENCES

1. Nishikawa, M., and Huang, L. (2001) *Hum. Gene Ther.* **12,** 861–870
2. Görlich. D., and Kutay, U. (1999) *Annu. Rev. Cell. Dev. Biol.* **15,** 607–660
3. Tseng, W. C., Haselton, F. R., and Giorgio, T. D. (1999) *Biochim. Biophys. Acta* **1445,** 53–64

4. Wilson, G. L., Dean, B. S., Wang, G., and Dean, D. A. (1999) *J. Biol. Chem.* **274,** 22025–22032
5. Cartier, R., and Reszka, R. (2002) *Gene Therapy* **9,** 157–167
6. Munkonge, F. M., Dean, D. A., Hillery, E., Griesenbach, U., and Alton, E. W. F. W. (2003) *Adv. Drug Deliv Rev.* **55,** 749–760
7. Fritz, J. D., Herweijer, H., Zhang, G., and Wolff, J. A. (1996) *Hum. Gene Ther.* **7,** 1395–1404
8. Vacik, J., Dean, B. S., Zimmer, W. E., and Dean, D. A. (1999) *Gene Therapy* **6,** 1006–1014
9. Dean, D. A., Dean, B. S., Muller, S., and Smith, L. C. (1999) *Exp. Cell Res.* **253,** 713–722
10. Längle-Rouault, F., Patzel, V., Benavente, A., Taillez, M., Silvestre, N., Bompard, A., Sczakiel, G., Jacobs, E., and Rittner, K. (1998) *J. Virol.* **72,** 6181–6185
11. Mesika, A., Grigoreva, I., Zohar, M., and Reich, Z. (2001) *Mol. Ther.* **3,** 653–667
12. Basner-Tschakarjan, E., Mirmohammadsadegh, A., Baer, A., and Hengge, U. R. (2004) *Gene Therapy* **11,** 765–774
13. Hillery, E., Munkonge, F. M., Xenariou, S., Dean, D. A., and Alton, E. W. F. W. (2006) *Anal. Biochem.* **352,** 169–175
14. Al-Mohanna, M. A., Al-Khodairy, F. M., Krezolek, Z., Bertilsson, P. A., Al-Houssein, K. A., and Aboussekhra, A. (2001) *Carcinogenesis* **22,** 573–578
15. Horton, P., Park, K. J., Obayashi, T., Fujita, N., Harada, H., Adams-Collier, C. J., and Nakai, K. (2007) *Nucleic Acids Res.* **35,** W585–W587
16. Karmirantzou, M., and Hamodrakas, S. J. (2001) *Protein Eng.* **14,** 465–472
17. Nair, R., and Rost, B. (2004) *Nucleic Acids Res.* **32,** W517–W521
18. Langer, T. (2000) *Histochem Cell Biol.* **113,** 455–465
19. Tsukahara, F., and Maru, Y. (2004) *J. Biol. Chem.* **279,** 8867–8872
20. Leung, S. M., and Hightower, L. E. (1997) *J. Biol. Chem.* **272,** 2607–2614
21. Okuno, Y., Imamoto, N., and Yoneda, Y. (1993) *Exp. Cell Res.* **206,** 134–142
22. Postel, E. H. (1999) *J. Biol. Chem.* **274,** 22821–22829
23. Ferda Percin, E., Ploder, L. A., Yu, J. J., Arici, K., Horsford, D. J., Rutherford, A., Bapat, B., Cox, D. W., Duncan, A. M., Kalnins, V. I., Kocak-Altintas, A., Sowden, J. C., Traboulsi, E., Sarfarazi, M., and McInnes, R. R. (2000) *Nat. Genet.* **25,** 397–401
24. Miller, A. M., and Dean, D. A. (2008) *Gene Therapy* **15,** 1107–1115
25. Kuramoto, T., Nishikawa, M., Thanaketpaisarn, O., Okabe, T., Yamashita, F., and Hashida, M. (2006) *J. Gene Med.* **8,** 53–62
26. Thanaketpaisarn, O., Nishikawa, M., Okabe, T., Yamashita, F., and Hashida, M. (2008) *J. Biotechnol.* **133,** 36–41
27. Jeffery, C. J. (1999) *Trends Biochem Sci.* **24,** 8–11
28. Kim, J. W., Zeller, K. I., Wang, Y., Jegga, A. G., Aronow, B. J., O'Donnell, K. A., and Dang, C. V. (2004) *Mol. Cell. Biol.* **24,** 5923–5936
29. Pickart, C. M. (2001) *Annu. Rev. Biochem.* **70,** 503–533